


Lyapunov Self-triggered Controller for Nonlinear Trajectory Tracking of Unicycle-type Robot

Carlos Santos* , Felipe Espinosa, Enrique Santiso, and David Gualda

Abstract: This paper focuses on the design and implementation of an aperiodic control of nonholonomic robots tracking nonlinear trajectories. The main objective of our controller is to reduce the number of updates while preserving control performance guarantees. To solve the problem in a more efficient way, we design two aperiodic control solutions, one to reach a target point and a second to track a predefined nonlinear trajectory. Unlike most previous work, our triggering condition only updates the controller when the time derivative of the Lyapunov function becomes non-negative, without taking into account the measurement error. Multiple simulated results with different initial conditions are included, showing how our control solution significantly reduces the need for communication in comparison with periodic and other aperiodic strategies while preserving a desired tracking performance. To validate the proposal experimental tests of each control technique with a P3-DX robot remotely controlled through an IEEE 802.11g wireless network are also carried out.

Keywords: Lyapunov-based controller, nonlinear trajectory-tracking, self-triggered, semiglobal practical stability.

1. INTRODUCTION

With the proliferation of Network Control Systems (NCS), greater functionality is expected because control loops no longer have at their disposal dedicated computational and communication resources [1]. In these systems, the performance depends not only on the designed control algorithm but also on resources scheduling in the shared network. This has motivated an increasing interest in techniques that avoid periodic implementations in favor of strategies based on the idea of sampling only when the system needs attention. These techniques employ information about the state of the system to update the control signal only when a certain condition is violated.

Two of the most well-known techniques are event-triggered (ETC) [1–6] and self-triggered control (STC) [7–11]. Self-triggered control is proactive, it predicts when the system will need to be updated. Thus, the controller determines the next update time from the last measurement. In contrast, ETC is reactive, the current state of the plant is constantly monitored in order to decide when the control must be updated. The basics of these controllers are introduced in [12] and a comparative study in [13].

The nonlinear aperiodic control is field with a great popularity in recent times, representative works of this in-

novative control technique are [10–12, 14, 15]. In [10] a STC that guarantees practical stability of a perturbed nonlinear system is presented. In [11] a STC for nonlinear systems perturbed by norm-bounded parameter uncertainties and disturbances is described. In [14], authors show that with a properly designed prediction horizon, the feasibility and stability of the proposed self-triggered model predictive control (MPC) algorithm can be guaranteed if the disturbance is bounded in a small enough area. In [15], authors present an ETC in which the triggering condition is checked in the control law itself instead of using a Lyapunov function, this reduces the complexity of computing the event. In [12] multiple works of ETC and STC applied to nonlinear systems are presented. However, unlike these previous works, this paper presents a triggering technique that is not based directly on the measurement error but on the function of Lyapunov, thus achieving greater times between samples without degrading the performance.

Previous works concerning event-based control of non-holonomic robots tracking nonlinear trajectories are [2, 4, 8, 9, 16]. In [2], an event-triggered nonlinear feedback law is designed and tested using a Khepera III robot and an IEEE 802.11g wireless network. However, communication between the robot and the remote center requires periodic updating to check the event triggering condition. In [8], a model predictive control framework combined

Manuscript received August 12, 2018; revised October 22, 2018, June 18, 2019, and September 11, 2019; accepted November 10, 2019. Recommended by Associate Editor Yingmin Jia under the direction of Editor Fumitoshi Matsuno.

Carlos Santos, Felipe Espinosa, Enrique Santiso, and David Gualda are with the Electronics Department, University of Alcalá. Engineering School, Campus Universitario, 28805 Alcalá de Henares, Spain (e-mails: {carlos.santos, felipe.espinosa, enrique.santiso, david.gualda}@uah.es).

* Corresponding author.

with a self-triggered mechanism for constrained uncertain systems is designed to control a simulated nonholonomic robot, but it needs continuous communication between the controller and the robot. In [16] a self-triggered MPC controller strategy for unicycle-type robots with coupled input constraint and bounded disturbances is presented. Stability is guaranteed by means of a Lyapunov function. However, only simulation results are presented due to the complexity of modelling and computing in a real application. In [9], adaptive self-triggered linear control is applied for trajectory tracking with a P3-DX robot; however, only the stability of the velocity control loop is guaranteed and the necessary velocity references are generated with the aid of a Mamdani fuzzy control solution.

The main contributions of the present paper are:

- 1) Design and implementation of a novel self-triggered Lyapunov-based control for nonlinear systems that guarantees practical stability. This triggering condition achieves a dual stability approach, when the Lyapunov function is greater than a predefined threshold, asymptotic stability is guaranteed and after that, the system is bounded on the given Lyapunov threshold level.
- 2) Comparison of our triggering mechanism with another one based on the measurement error [10] and with a periodic implementation. This way we remark the improvement achieved in the relation between number of updates and control performance.
- 3) Evaluation of our triggering mechanisms for approaching and nonlinear trajectory tracking in a real-life scenario where a P3-DX robot is remotely controlled through an IEEE 802.11g wireless network.

The rest of the paper is organized as follows: Section 2 presents the application problem: the trajectory tracking of a nonholonomic robot. Section 3 revisits the nonlinear aperiodic control problem. Section 4 describes our nonlinear event-triggered strategy. Section 5 validates our proposal with simulation results. In Section 6, we describe the experimental scenario and present the results. Finally, Section 7 summarizes the contributions of this paper.

2. MOTIVATION

A common problem concerning the remote guidance of vehicles is the design of control laws to reach and follow a time-parameterized reference. This problem is especially challenging when considering nonlinear trajectories and nonholonomic vehicles [17]. This is the case of differential-drive robots, which only possess two actuation variables (linear velocity and angular velocity) for locomotion control, whereas the pose of the mobile unit is characterized by three degrees of freedom.

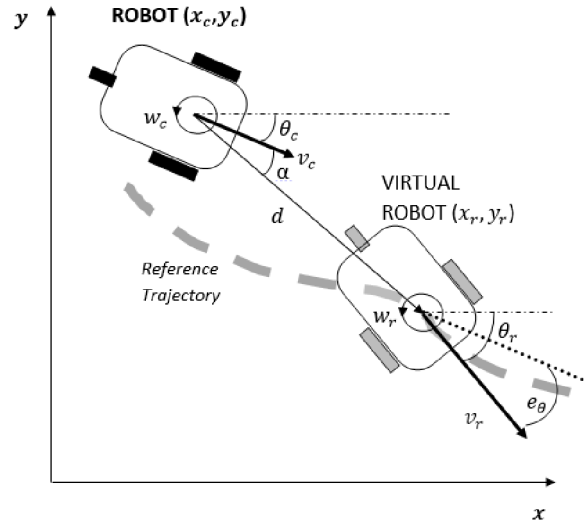


Fig. 1. Main variables describing the dynamics of the trajectory tracking stage, where a virtual robot represents the reference pose: d is the distance error calculated from the robot point to the virtual reference point, α is the orientation error with respect to the target point, e_θ is the orientation error between the desired orientation to follow the trajectory (θ_r) and the current orientation of the robot (θ_c).

2.1. Robot model

Fig. 1 shows the main elements involved in the trajectory tracking problem. A virtual robot tracking the trajectory perfectly under test conditions serves as the reference (x_r, y_r, θ_r) to be followed by the real robot (x_c, y_c, θ_c).

The kinematic equations of the robots [18] are:

$$\begin{aligned} \dot{x}_p(t) &= v_p(t) \cos(\theta_p(t)), & \dot{y}_p(t) &= v_p(t) \sin(\theta_p(t)), \\ \dot{\theta}_p(t) &= w_p, & p &\in \{c, r\}, \end{aligned} \quad (1)$$

where v_p is the linear velocity, w_p is the angular velocity, the subindex p means both current or reference variable.

The distance error d and the orientation error α with respect to the target point [18] are given by:

$$\begin{aligned} d(t) &= \sqrt{(x_r(t) - x_c(t))^2 + (y_r(t) - y_c(t))^2}, \\ \alpha(t) &= \text{atan2}(y_r(t) - y_c(t), x_r(t) - x_c(t)) - \theta_c(t). \end{aligned} \quad (2)$$

where $\text{atan2}(y, x)$ returns the four-quadrant inverse tangent (\tan^{-1}) of y and x , which must be real.

Prior works of aperiodic control [2, 8] used Cartesian coordinates. However, when the robot is localized with a set of Cartesian coordinates, according to the limitations indicated by Brockett's result [19], the target pose cannot be reached asymptotically through smooth and time-invariant feedback control laws. For this reason, we decide to use polar coordinates. Because this coordinate system

makes it possible to represent the problem in a simpler way and in this form to design a control strategy that allows smooth stabilization [20].

Taking into account the kinematic model (1) in polar coordinates [20], the distance and orientation errors result in:

$$\begin{aligned} \dot{d}(t) &= -v_c(t) \cos(\alpha(t)) + v_r(t) \cos(\alpha(t) - e_\theta(t)), \\ \dot{\alpha}(t) &= -w_c(t) + v_c(t) \frac{\sin(\alpha(t))}{d(t)} \\ &\quad - v_r(t) \frac{\sin(\alpha(t) - e_\theta(t))}{d(t)}, \\ \dot{e}_\theta(t) &= w_r(t) - w_c(t); \quad e_\theta(t) := \theta_r(t) - \theta_c(t). \end{aligned} \quad (3)$$

Remark 1: The polar coordinate transformation is only valid for non-zero values of the distance error d , as for $d = 0$, the angle α is not defined [21]. This singular point leads to a discontinuity in the control law. To avoid this, if $d = 0$ (i.e. the target is reached); we define $\alpha = 0$.

2.2. Problem statement

The problem studied in this paper is the path-following performance of a robot linked to a remote controller via a wireless channel. In the first stage, the robot has to approach the starting point of the path (target point); then, the remote controller switches to a control law to track the trajectory. In the approach stage, the objective is to reduce the distance error to the target point up to a given threshold. In the tracking stage, the distance and orientation errors are assessed taking as reference the movement of a virtual robot tracking the known trajectory perfectly. The network to communicate the robot and the remote center is assumed to be shared with other control tasks. For this reason, the main objective of this work is to reduce the wireless channel's load. The main contribution is the use of a novel triggering condition based only on the Lyapunov function and its time derivative, without taking into account the measurement error. With this less conservative triggering condition we enlarge the inter-execution times compared to previous aperiodical strategies based on measurement error [4, 10, 22, 23].

3. NONLINEAR APERIODIC CONTROL

In this section, we present the fundamentals of nonlinear aperiodic control solutions.

Notation: The Euclidean norm of vector $\|v\|$ is indicated by $v \in \mathbb{R}^n$. Given a signal $s : \mathbb{R}^+ \rightarrow \mathbb{R}^n$, it is denoted with $\|s\|_{\mathcal{L}_{\infty,k}} := \sup_{t \geq t_k} \|s(t)\|$. A function is said to be of class $C^0(\mathcal{D}_x)$ if it is continuous over \mathcal{D}_x , and it is said to be $C^l(\mathcal{D}_x)$, $l > 0$ if its derivatives are of class $C^{l-1}(\mathcal{D}_x)$. A continuous function $\gamma : [0, a[\rightarrow +\infty, a > 0$ is said to be of class \mathcal{K} if it is strictly increasing and $\gamma(0) = 0$. The Lipschitz constant of a function f is represented by L_f .

Now, the problem formulation of aperiodic control applied to nonlinear systems is introduced. Consider an autonomous nonlinear control system:

$$\dot{\xi}(t) = f(\xi(t), u(t)), \quad (4)$$

where $\xi(t) \in \mathcal{D}_x \subset \mathbb{R}^{n_x}$ and $u(t) \in \mathcal{D}_u \subset \mathbb{R}^{n_u}$, both domains containing the origin.

Assumption 1: There exists a differentiable state feedback law $K : \mathcal{D}_x \rightarrow \mathcal{D}_u$ such that the origin of the closed-loop continuous system

$$\dot{\xi}(t) = f(\xi(t), K(\xi(t))) \quad (5)$$

is the unique locally asymptotically stable equilibrium point in \mathcal{D}_x .

From Assumption 1, converse theorems [24, 25] ensure the existence of a Lyapunov function $V(\xi(t))$ for the system (5) such that:

$$\begin{aligned} \underline{\gamma}(\|\xi(t)\|) &\leq V(\xi(t)) \leq \bar{\gamma}(\|\xi(t)\|), \\ \dot{V}(\xi(t)) &= \frac{\partial V(\xi(t))}{\partial \xi} f(\xi(t), K(\xi(t))) \\ &\leq -\gamma_1(\|\xi(t)\|), \\ \left\| \frac{\partial V(\xi(t))}{\partial \xi} \right\| &\leq \gamma_2(\|\xi(t)\|), \end{aligned} \quad (6)$$

with $\underline{\gamma}, \bar{\gamma}, \gamma_1, \gamma_2$ are \mathcal{K} -class functions.

Assumption 2: Assume that:

- 1) The function $f \in C^l(\mathcal{D}_\xi \times \mathcal{D}_u)$, with $l \geq 3$.
- 2) The functions $\underline{\gamma}, \gamma_1 \in \mathcal{K}$ in (6) are such that $\underline{\gamma}^{-1}, \gamma_1$ are Lipschitz continuous on the working compact set (\mathcal{D}_ξ) . The Lipschitz constants on \mathcal{D}_ξ of functions $\underline{\gamma}^{-1}$ and γ_1 are represented by $L_{\underline{\gamma}^{-1}}$ and L_{γ_1} respectively.

The control signal is implemented in a zero-order hold (ZOH) fashion, that is, the controller is recomputed at times t_k with fresh measurements, and the control input is kept constant until a new measurement is received, i.e.:

$$u(t) = K(\xi(t_k)), \quad t \in [t_k, t_{k+1}[, \quad k \in \mathbb{N}. \quad (7)$$

With this implementation, the sampled-data system dynamics are given by:

$$\dot{\xi}(t) = f(\xi(t), K(\xi(t_k))), \quad t \in [t_k, t_{k+1}[, \quad k \in \mathbb{N}. \quad (8)$$

4. LYAPUNOV BASED SELF-TRIGGERED CONTROL PROPOSAL

In this section, a self-triggering condition assuming that the full state information is available at the measurement instants is proposed. The triggering condition is based on the Lyapunov function that describes the stability of the closed loop system with the sample and hold implementation and its time derivative.

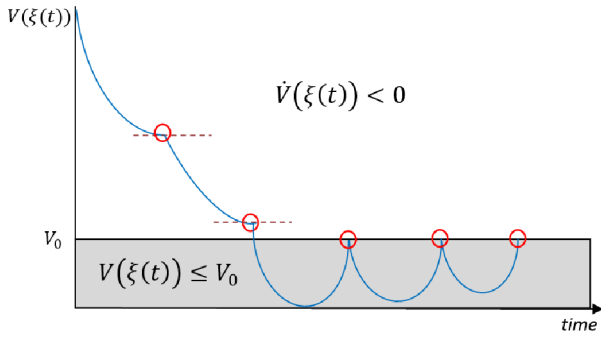


Fig. 2. Graphical description of the proposed self-triggering condition (9). When the Lyapunov function is greater than V_0 , every time the derivative of the Lyapunov function is non negative the system is updated. When the system converges to the invariant set defined by V_0 , the system is updated when the Lyapunov function hits the threshold V_0 .

Theorem 1: Suppose that Assumptions 1 and 2 hold for \mathcal{D}_ξ and $\xi(t_0) \in \mathcal{D}_\xi$. If the control signal is updated according to the following triggering condition

$$t_{k+1} = \min\{t > t_k \mid (\dot{V}(\xi(t)) \geq 0 \wedge V(\xi(t)) \geq V_0)\}, \quad (9)$$

the system (8) converges asymptotically to the bounded set \mathcal{D}_{V_0} , where $\mathcal{D}_{V_0} = \{\xi(t) \mid V(\xi(t)) < V_0\}$.

Fig. 2 illustrates the triggering mechanism based on the Lyapunov function.

Proof: By Theorem 3.2 of [26] the triggering condition (9) enforces semiglobal practical stability of the system (8), as long no Zeno executions are presented.

In order to show that the proposed triggering condition does not introduce Zeno executions, Theorem 4.1 of [10] is employed to show that a strictly positive minimum dwell-time between triggering controller updates. In [10], the error function $g(t)$ is defined as:

$$g(t) := f(\xi(t), K(\xi(t_k))) - f(\xi(t), K(\xi(t))), \quad t \in [t_k, t_{k+1}[, k \in \mathbb{N}, \quad (10)$$

and the dynamics of the sample-data system (8) is rewritten as:

$$\dot{\xi}(t) = f(\xi(t), K(\xi(t_k))) + g(t), \quad t \in [t_k, t_{k+1}[, k \in \mathbb{N}. \quad (11)$$

The following sampling rule:

$$t_{k+1} = \min\{t > t_k \mid \|g(t)\| > e_{V_0}\}, \quad (12)$$

is proposed by [10]. It ensures semiglobal practical stability of the closed-loop system for any $e_{V_0} > 0$ and guarantees a positive minimum dwell-time if Assumptions 1

and 2 hold for any (arbitrarily large) compact set \mathcal{D}_ξ and $\xi(t_0) \in \mathcal{D}_\xi$.

It can be shown that condition (9) presents equal or greater inter-execution times than (12) for some selection of $e_{V_0} > 0$, then by virtue of Theorem 4.1 of [10], the desired result is obtained: the existence of a strictly positive minimum dwell-time, and thus no Zeno execution is possible. Observe that:

$$\begin{aligned} \dot{V}(\xi(t)) &= \frac{\partial V(\xi(t))}{\partial \xi} f(\xi(t), K(\xi(t_k))) \\ &= \frac{\partial V(\xi(t))}{\partial \xi} f(\xi(t), K(\xi(t))) \\ &\quad + \frac{\partial V(\xi(t))}{\partial \xi} (f(\xi(t), K(\xi(t_k))) \\ &\quad - f(\xi(t), K(\xi(t)))) \\ &\leq -\gamma_1(\|\xi(t)\|) + \gamma_2(\|\xi(t)\| \|g(t)\|), \end{aligned} \quad (13)$$

which together with (12) implies:

$$\dot{V}(\xi(t)) \leq -\gamma_1(\|\xi(t)\|) + \gamma_2(\|\xi(t)\|_{\mathcal{L}_{\infty,k}}) e_{V_0}. \quad (14)$$

Thus, (12) enforces the following implication:

$$\dot{V}(\xi(t)) < 0 \quad \forall t, \quad \text{if } \|\xi(t)\| > \gamma_1^{-1}(\gamma_2(\|\xi(t)\|_{\mathcal{L}_{\infty,k}}) e_{V_0}). \quad (15)$$

Inspecting the triggering condition (9) it is observed that it *only* demands new updates if:

$$\dot{V}(\xi(t)) \geq 0 \quad \wedge \quad V(\xi(t)) > V_0, \quad (16)$$

thus from (6) it is proven that (9) forces updates when:

$$\dot{V}(\xi(t)) \geq 0 \quad \wedge \quad \|\xi(t)\| \geq \bar{\gamma}^{-1}(V_0). \quad (17)$$

Select now an e_{V_0} such that:

$$\gamma_1^{-1}(\gamma_2(\|\xi(t)\|_{\mathcal{L}_{\infty,k}}) e_{V_0}) \leq \bar{\gamma}^{-1}(V_0). \quad (18)$$

Such an $e_{V_0} > 0$ always exists as long as $\|\xi(t)\|_{\mathcal{L}_{\infty,k}}$ is upper bounded, from the properties of \mathcal{K}_∞ functions and $V_0 > 0$. Note that $\|\xi(t)\|_{\mathcal{L}_{\infty,k}}$ is upper bounded as $V(\xi(0)) < \infty$ and thus due to (9) $V(\xi(t)) < \infty$ for all positive times, which by (6) implies the required boundedness.

Finally, by virtue of (18) it is proven that when (17) takes place the triggering condition from (12) is certainly violated. \square

Remark 2: To find a dwell-time, Theorem 4.1 of [10] is used because the triggering condition (9) presents no lower inter-execution times than (12) outside of the bounded set defined by \mathcal{D}_{V_0} . This is due to the triggering condition (9) that depends directly on the Lyapunov time derivative and not on the absolute value of the measurement error as (12).

4.1. Controller for reaching a target point

This is a special case of the problem described in Fig. 1, in which, $v_r(t) = 0$, $w_r(t) = 0$ and $\theta_r(t) \in [-\pi, \pi]$ [18].

Considering the kinematic model described in (2) and (3) and a fixed target point, the evolution of the distance and orientation errors in polar coordinates, are defined as:

$$\begin{aligned} \dot{d}(t) &= -v_c(t) \cos(\alpha(t)), \\ \dot{\alpha}(t) &= -w_c(t) + v_c(t) \frac{\sin(\alpha(t))}{d(t)}. \end{aligned} \quad (19)$$

The designed controllers are based on Lyapunov functions. The following control laws are applied:

$$v_c(t) = K_{v1} \cos(\alpha(t))d(t), \quad (20)$$

$$w_c(t) = K_{w1} \alpha(t) + K_{v1} \cos(\alpha(t)) \sin(\alpha(t)), \quad (21)$$

where $K_{v1} > 0$ and $K_{w1} > 0$ are the approaching control gains, and the following equation is a Lyapunov function for the closed-loop system (19):

$$V(t) = \frac{1}{2} \lambda d(t)^2 + \frac{1}{2} \alpha(t)^2, \quad (22)$$

where λ is an adjustment factor greater than 0.

The time derivative \dot{V} along (19) is given by:

$$\dot{V} = -dv_c \cos(\alpha) + \alpha \left(-w_c + v_c \frac{\sin(\alpha)}{d} \right), \quad (23)$$

which leads to the following expression ensuring a negative value for the \dot{V} function:

$$\dot{V} = -K_{v1} d^2 \cos^2(\alpha) - K_{w1} \alpha^2 < 0. \quad (24)$$

4.2. Controller for nonlinear trajectory tracking

In this section the controller applied to track the nonlinear trajectory is described. As prescribed in [20], the following linear and angular control laws are applied to (3):

$$v_c(t) = K_{v2} d(t) \cos(\alpha(t)) + v_r(t) \cos(e_\theta(t)), \quad (25)$$

$$\begin{aligned} w_c(t) &= \dot{\theta}_{md}(t) + v_{md}(t) (K_{w2} (v_{ls}(t) \sin(\alpha(t)) \\ &\quad + v_r(t) \sin(e_\theta(t))) + d(t) \sin(\alpha(t))), \end{aligned} \quad (26)$$

where θ_{md} is the modified desired heading angle:

$$\begin{aligned} \theta_{md}(t) &:= \text{atan2} \left(\frac{K_{v2} d(t) \sin(\alpha(t) - e_\theta(t))}{v_r(t) + K_{v2} d(t) \cos(\alpha(t) - e_\theta(t))} \right) \\ &\quad + \theta_r(t), \end{aligned} \quad (27)$$

and v_{md} is the modified desired linear velocity:

$$\begin{aligned} v_{md}(t) &:= \sqrt{v_r(t)^2 + (K_{v2} d(t))^2 + 2v_r(t) K_{v2} d(t) \cos(\alpha(t) - e_\theta(t))}, \\ &\quad (28) \end{aligned}$$

being $K_{v2} > 0$ and $K_{w2} > 0$ the tracking gains associated with the linear and angular velocities. The following equation is a Lyapunov function for the resulting closed-loop system:

$$V(t) = \frac{1}{2} d(t)^2 + 1 - \cos(\theta_{md}(t) - \theta_c(t)) \quad (29)$$

is a Lyapunov function for the system (3). The time derivative of V is:

$$\dot{V} = -K_{v2} d^2 - K_{w2} (K_{v2} d \sin(\alpha) + v_r \sin(e_\theta))^2 < 0. \quad (30)$$

Remark 3: When the STC computes the next update instant t_{k+1} , all reference velocities, $v_r(t)$ and $w_r(t)$, are assumed to be piecewise constant between the current time t_k and the next update time t_{k+1} . However, if a change in reference signals is detected the next update instant t_{k+1} is recalculated.

5. SIMULATION RESULTS

In this section different simulation results are presented. First, the control technique to reach a point is tested. Next, the trajectory tracking simulation results are shown.

In order to validate the proposal, a comparison is presented with different control implementations: a continuous strategy, two periodic implementations, and three ETC with the triggering condition described in (12) but different thresholds.

5.1. Reaching a point

Fig. 3 describes the kinematic model of a differential wheeled robot, with the control parameters $\lambda = 0.01$, $K_{v1} = 0.1$, $K_{w1} = 0.1$ and $V_0 = 10^{-2}$. The robot is initially positioned with the opposite orientation required to reach the target. The initial location (O) is $(x_c, y_c, \theta_c) = (-10, 0, \pi)$ and the target (D) is at the coordinate origin with $\theta_r \in [-\pi, \pi]$ (see Fig. 3).

Fig. 4 compares the Lyapunov functions applying both the self-triggered strategy and the continuous time strategy. Note that in this case, the aperiodic one achieves a better performance, reaching the equilibrium point faster than the continuous strategy. The discrete update instants are also shown, and as can be seen, the system reaches the equilibrium point after only four updates.

A statistical study is also carried out to better characterize the validation procedure. The study consists of 100 simulations of each implementation. A random combination for initial pose conditions has been chosen. Table 1 summarizes the average and the standard deviation of performance and updates of each control technique. For the case under study, our STC solution provides the best results with the lowest update and performance average values. The results for STC (12) are also presented, in order

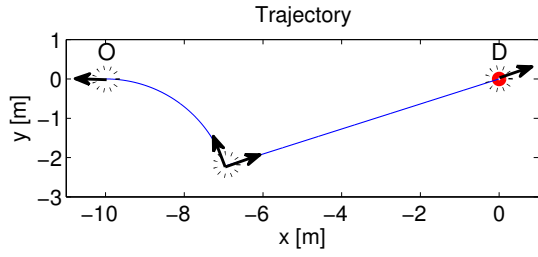


Fig. 3. Example of nonlinear trajectory generated by the reaching a point strategy; the robotic unit departs from the original pose O to reach the destination point D .

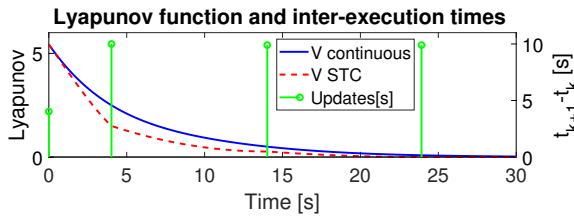


Fig. 4. Comparison of Lyapunov functions for the continuous control strategy (blue line), the STC strategy (red line) and the update times (green color).

Table 1. Comparison of the average (AVG) and the standard deviation (STD) values of update number (Upd) and RMS value of distance after 100 simulation results concerning the different control strategies for reaching a point, including the triggering conditions (12) and (9).

	AVG Upd	STD Upd	AVG d_{RMS} (m)	STD d_{RMS} (m)
Continuous	-	-	73.33	46.16
Periodic $T_s = 100$ ms	800	0	73.04	45.97
Periodic $T_s = 1$ s	80	0	70.48	44.35
STC (12) $e_{V_0} = 0.005$	48.15	11.93	70.98	45.12
STC (12) $e_{V_0} = 0.25$	11.57	1.80	64.94	41.76
STC (12) $e_{V_0} = 1$	8.59	1.3	71.35	43.89
Our proposal STC (9)	2.5	0.52	58.55	40.31

to find the best result for this technique different threshold values (e_{V_0}) are simulated and the best three are presented. This technique achieves also better results than the periodic implementation.

5.2. Trajectory tracking

A simulation example based on the previously mentioned robot kinematic model is presented, with control

parameters $K_{v2} = 0.8$, $K_{w2} = 0.1$ and $V_0 = 10^{-2}$. The initial robot location (O_R) is $(x_c, y_c, \theta_c) = (0.1, 3, -\frac{\pi}{2})$ and the initial trajectory point (O_T) is $(x_r, y_r, \theta_r) = (0, 2, \pi)$. The nonlinear trajectory is shown in Fig. 5. The robotic unit starts from the origin O_R and stops at the destination point D . The designed control shows how the self-triggered controller greatly reduces the number of changes in the control signals remotely applied to the robot, while also achieving a good performance.

Using the aperiodic technique presented in Section 4, the controller needs 65 updates for proper trajectory tracking over 80 seconds of simulation. The analysis of the Lyapunov functions presented in Fig. 6 shows that our self-triggered controller achieves a better performance than the continuous.

As in the previous section, a statistical study is carried out to better characterize the validation procedure, including 100 simulations of each implementation. A random combination of initial pose conditions has been chosen. Table 2 summarizes the average and the standard deviation of performance and updates of each control technique. It can be observed that the better results are achieved with the STCs, the aperiodic controllers present a good balance between the number of updates and the performance. In this particular case our controller obtains the best average performance and the STC with the triggering condition (12) the lowest number of updates when the threshold is $e_{V_0} = 0.25$.

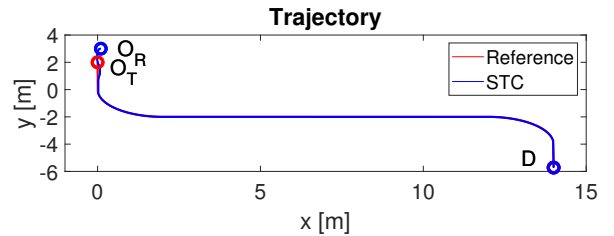


Fig. 5. The nonlinear trajectory tracking of the robotic unit implementing the designed STC. The robot starts from the initial location O_R and follows the trajectory from the origin O_T to the destination point D .

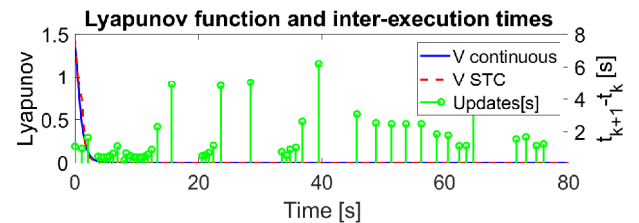


Fig. 6. Comparison of continuous and STC Lyapunov functions, as well as the aperiodic update times.

Table 2. Comparison of the average (AVG) and the standard deviation (STD) values of update number (Upd) and RMS value of distance after 100 simulation results concerning the different control strategies for trajectory tracking, including the triggering conditions (12) and (9).

	AVG Upd	STD Upd	AVG d_{RMS} (m)	STD d_{RMS} (m)
Continuous	-	-	4.08	1.65
Periodic $T_s=100$ ms	800	0	4.14	1.68
Periodic $T_s=1$ s	80	0	4.91	1.82
STC (12) $e_{v_0} = 0.005$	114.52	10.37	3.99	1.78
STC (12) $e_{v_0} = 0.05$	49.63	5.48	3.94	2.03
STC (12) $e_{v_0} = 0.25$	45.03	14.59	5.98	2.90
Our proposal STC (9)	81.64	24.38	2.81	2.06

6. EXPERIMENTAL RESULTS

The tests were performed using a Pioneer P3DX robot with additional electronics such as it is described in [27]. A mini PC (Model number NUC5i3RYH) with Intel Core i3 processor and 4 GB of RAM implemented the remote centre. The remote centre and the robot were running Ubuntu 12.04 as their operating system. The wireless router chosen for this application is the Buffalo WHR-HP-G54, which is in compliance with standards IEEE802.11b/.11g, some specifications and parameter configuration are: 11 frequency channels, transmission rate of 125 Mbps, WPA-PSK and 128 bits WPE and 4 LAN ports. The client device chosen to connect to the router is the WLI-TX4-G54HP. Fig. 7 shows the complete experimental platform described in this section.

P3-DX robot state-space model is detailed in [9, 28]. Among the practical aspects to be considered are: robot

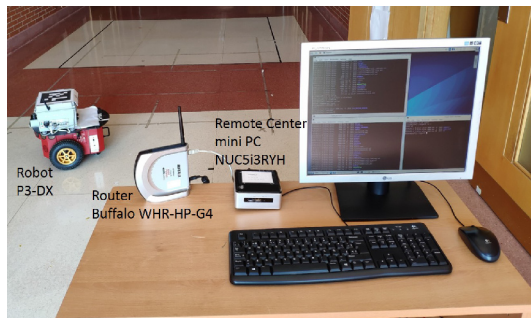


Fig. 7. Complete experimental platform: remote center (mini PC NUC5i3RYH), robot (Pioneer P3-DX) and wireless router (WHR-HP-G4).

dynamics [29] and network channel delay [28]. A quickly enough periodic velocity servosystem is locally implemented in the robot, thus the robot dynamics can be neglected. In addition, we use the network delay compensation presented in [28] to compensate the robot's reaction time and the variable network delays.

An error in the prediction due to uncertainties of the real system is also assumed but this is the reason a triggering condition that guarantees practical stability instead asymptotic or exponential stability is chosen.

Fig. 8 shows the structure of the implemented approach and tracking self-triggered control. The remote PC and the P3-DX are nodes of the same wireless network. The PC carries out two main tasks: updating the velocity vector ($v_c(t_k), w_c(t_k)$) to track the desired trajectory, and computing the next sampling instant (t_{k+1}). Meanwhile, the self-triggered scheduler is responsible for deciding when the system state vector is updated and when the control action is applied. It is clear that the higher the inter-executions interval, the lower the load on the wireless channel.

The Lyapunov-based controller switches between the approach and tracking control alternatives. On the one hand, when the robot is farther than a meter from the desired trajectory, the main objective is to converge to the path, and for this the target-reaching strategy (Section 4.1) is selected. On the other hand, when the robot is closer than a meter from the path, the trajectory-tracking strategy (Section 4.2) is applied. This allows the designer to focus each controller on the specific objective by defining

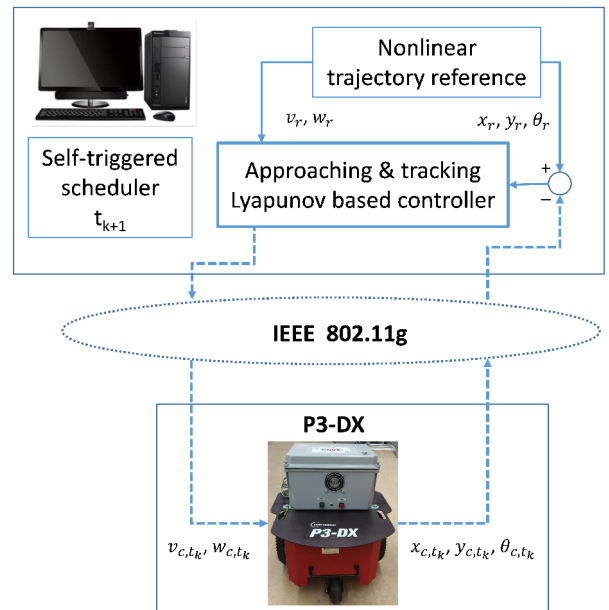


Fig. 8. Detail of the general architecture, where a desktop computer remotely controls a P3-DX robot. The PC and the robot are connected through the wifi network of the test environment.

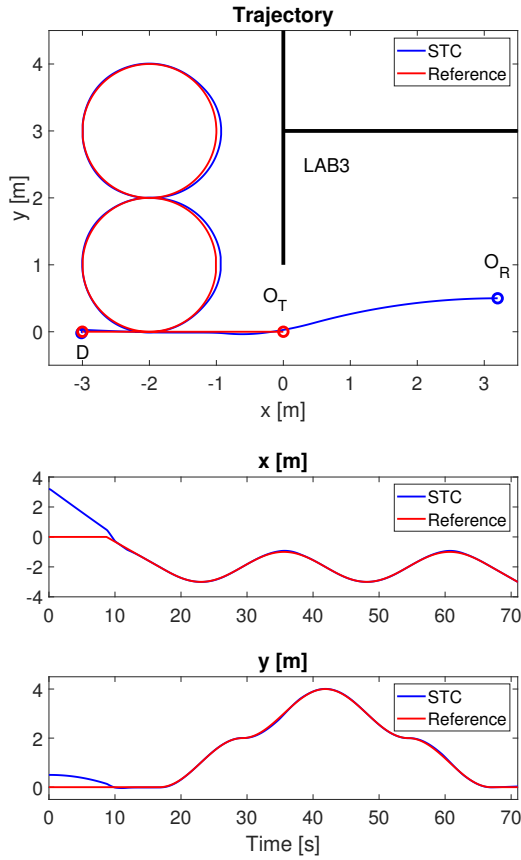


Fig. 9. Experimental validation of the aperiodic remote control for nonlinear trajectory tracking. The robot starts from the initial position O_R in LAB1, reaches the initial trajectory point O_T and follows (blue line) the eight-shaped path (red line) in the corridor, to the destination point D . Top picture: 2D trajectories, reference and registered ones. Bottom picture: time response of x and y coordinates registered along the route.

the triggering function to achieve a good trade-off between performance and number of updates.

As an example, an eight-shaped trajectory has been generated and implemented in the laboratory area of the Engineering School at the University of Alcalá. The robot departs from the initial position O_R in LAB1, and follows a circular route that starts at O_T and finishes at D , the start time of the trajectory is considered when the controller switches to the tracking control strategy. Fig. 9 illustrates the 2D reference and trajectory tracking resulting of the experimental test as well as the time response of x and y coordinates along the route. As can be seen, the first part is associated with the target-reaching problem, and the second with the trajectory tracking problem.

Fig. 10 shows the temporal evolution of linear and angular velocities: those calculated by the Lyapunov-based

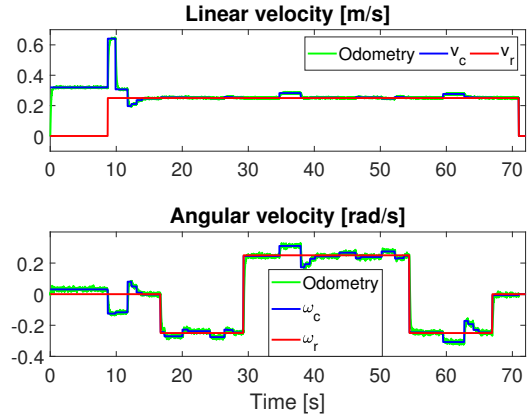


Fig. 10. Comparison of linear (top side) and angular (bottom side) velocities: reference (red color), control (blue) and measured by odometry (green).

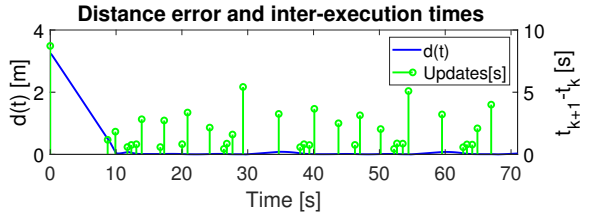


Fig. 11. Distance error $d(t)$ (blue color), described in 2, and inter-executions times (green) where the control action is updated.

controller (v_c, w_c), the references (v_r, w_r) provided by the trajectory generator, and the ones registered locally by the robot.

Fig. 11 allows to evaluate the temporal evolution of the distance error (Equation 2) and the inter-execution times. Over the 72 seconds of the experiment, the P3-DX reached the destination point D with only 35 updates of the control law and the same number of bidirectional accesses to the wireless channel.

To validate the proposal, the same experimental test are also carried out with the different control implementations presented in Section 5: three periodic implementations, and three STC with the triggering condition described in (12) but different threshold. Table 3 presents the performance results and updates of each control technique, a detailed analysis of the results obtained in the approach to the trajectory phase and in the trajectory tracking strategy are also presented. It can be observed that the better results are achieved with the STCs. In this particular case our controller obtains the best average performance and the lowest number of updates. The switch time indicates how long it takes to reach the O_T point with up to 1m distance error. In this case, it can be appreciated how our controller manages to do it in less time, with the best performance and with a single sample.

Table 3. Comparison of update number and RMS value of distance concerning the different control strategies for reaching a point and trajectory tracking, including the triggering conditions (12) and (9).

	Periodic Ts= 1 ms	Periodic Ts= 100 ms	Periodic Ts= 1 s	Our proposal STC (9)
Updates	81894	818	81	36
d_{RMS} (m)	28.930	28.775	27.602	18.244
Switch time	18.694	18.60	17.75	8.722
Updates approaching	18694	186	17	1
d_{RMS} (m) approaching	27.713	27.579	26.370	16.4971
Updates tracking	63200	632	64	35
d_{RMS} (m) tracking	1.217	1.196	1.232	1.746
	STC (12) $e_{v_0}=0.005$	STC (12) $e_{v_0}=0.25$	STC (12) $e_{v_0}=1$	Our proposal STC (9)
Updates	144	147	42	36
d_{RMS} (m)	28.352	26.112	23.202	18.244
Switch time	17.83	16.01	13.72	8.722
Updates approaching	21	7	3	1
d_{RMS} (m) approaching	26.634	24.418	21.312	16.4971
Updates tracking	123	40	39	35
d_{RMS} (m) tracking	1.718	1.694	1.897	1.746

7. CONCLUSIONS

A novel aperiodic nonlinear trajectory tracking controller for nonholonomic mobile robots is presented. To take advantage of different controllers, the solution includes two stages: approaching the trajectory from an arbitrary initial pose, and trajectory tracking to a destination, assuming a unicycle kinematic model. A specific aperiodic Lyapunov-based control solution is designed, that guarantees semiglobal practical stability and avoids Zeno executions. In order to achieve longer inter-execution times than previous works on aperiodic control, we design a triggering condition build from a system Lyapunov function. The main advantage of our self-triggered control is that we maintain the control signal unless the time derivative of the Lyapunov function becomes non-negative. This ensures that updates only take place when they are necessary. A comparison with different periodic and aperiodic alternatives has been tested. Validation by simulation and experimentation with a real robot confirms that our aperiodic solution leads to good target approach and trajectory tracking performance with a significant reduction in the number of control updates, and therefore a substantial reduction in wireless channel load.

REFERENCES

- [1] D. Liu and F. Hao, "Decentralized event-triggered control strategy in distributed networked systems with delays," *International Journal of Control, Automation and Systems*, vol. 11, pp. 33-40, Feb. 2013.
- [2] R. Postoyan, M. C. Bragagnolo, E. Galbrun, J. Daafouz, D. Netic, and E. B. Castelan, "Nonlinear event-triggered tracking control of a mobile robot: design, analysis and experimental results," *IFAC Proceedings Volumes*, vol. 46, pp. 318-323, Jan. 2013.
- [3] C. Santos, M. Martinez-Rey, F. Espinosa, A. Gardel, and E. Santiso, "Event-based sensing and control for remote robot guidance: An experimental case," *Sensors*, vol. 17, no. 9, 2017.
- [4] X. Chen, F. Hao, and B. Ma, "Periodic event-triggered cooperative control of multiple non-holonomic wheeled mobile robots," *IET Control Theory Applications*, vol. 11, no. 6, pp. 890-899, 2017.
- [5] D. Zhao, T. Dong, and W. Hu, "Event-triggered consensus of discrete time second-order multi-agent network," *International Journal of Control, Automation and Systems*, vol. 16, pp. 87-96, Feb. 2018.
- [6] Z. Tang, "Event-triggered consensus of linear discrete-time multi-agent systems with time-varying topology," *International Journal of Control, Automation and Systems*, vol. 16, pp. 1179-1185, Jun 2018.
- [7] M. Mazo, A. Anta, and P. Tabuada, "On self-triggered control for linear systems: Guarantees and complexity," in *2009 European Control Conference (ECC)*, pp. 3767-3772, Aug 2009.
- [8] A. Eqtami, S. Heshmati-alamdari, D. V. Dimarogonas, and K. J. Kyriakopoulos, "Self-triggered model predictive control for nonholonomic systems," *Proc. of European Control Conference (ECC)*, pp. 638-643, July 2013.
- [9] C. Santos, M. Mazo, and F. Espinosa, "Adaptive self-triggered control of a remotely operated p3-dx robot: Simulation and experimentation," *Robotics and Autonomous Systems*, vol. 62, no. 6, pp. 847-854, 2014.
- [10] U. Tiberi and K. Johansson, "A simple self-triggered sampler for perturbed nonlinear systems," *Nonlinear Analysis: Hybrid Systems*, vol. 10, pp. 126-140, 2013. Special Issue related to {IFAC} Conference on Analysis and Design of Hybrid Systems (ADHS 12).
- [11] M. D. D. Benedetto, S. D. Gennaro, and A. D'Innocenzo, "Digital self triggered robust control of nonlinear systems," *Proc. of 50th IEEE Conference on Decision and Control and European Control Conference*, pp. 1674-1679, Dec. 2011.
- [12] W. P. M. H. Heemels, K. H. Johansson, and P. Tabuada, "An introduction to event-triggered and self-triggered control," *Proc. of IEEE 51st IEEE Conference on Decision and Control (CDC)*, pp. 3270-3285, Dec 2012.
- [13] C. Santos, F. Espinosa, E. Santiso, and M. Martinez-Rey, "A simplified event-triggering condition non-dependent on measurement error," *Proc. of 3rd International Conference on Event-Based Control, Communication and Signal Processing (EBCCSP)*, pp. 1-6, May 2017.

- [14] Y. Su, Q. Wang, and C. Sun, "Self-triggered robust model predictive control for nonlinear systems with bounded disturbances," *IET Control Theory Applications*, vol. 13, no. 9, pp. 1336-1343, 2019.
- [15] N. Marchand, J. Martinez, S. Durand, and J. Guerrero-Castellanos, "Lyapunov event-triggered control: a new event strategy based on the control," *IFAC Proceedings Volumes*, vol. 46, no. 23, pp. 324-328, 2013.
- [16] Q. Cao, Z. Sun, Y. Xia, and L. Dai, "Self-triggered mpc for trajectory tracking of unicycle-type robots with external disturbance," *Journal of the Franklin Institute*, vol. 356, no. 11, pp. 5593-5610, 2019.
- [17] F. Heidari and R. Fotouhi, "A human-inspired method for point-to-point and path-following navigation of mobile robots," *Journal of Mechanisms and Robotics*, vol. 7, pp. 041025-041025-18, July 2015.
- [18] M. Aicardi, G. Casalino, A. Bicchi, and A. Balestrino, "Closed loop steering of unicycle like vehicles via lyapunov techniques," *Robotics Automation Magazine, IEEE*, vol. 2, pp. 27-35, Mar 1995.
- [19] R. W. Brockett, "Asymptotic stability and feedback stabilization," *Differential Geometric Control Theory*, pp. 181-191, Birkhauser, 1983.
- [20] M. Amoozgar and Y. Zhang, "Trajectory tracking of wheeled mobile robots: A kinematical approach," *Proc. of IEEE/ASME International Conference on Mechatronics and Embedded Systems and Applications (MESA)*, pp. 275-280, July 2012.
- [21] Z. Wang and Y. Liu, "Visual regulation of a nonholonomic wheeled mobile robot with two points using lyapunov functions," *Proc. of International Conference on Mechatronics and Automation (ICMA)*, pp. 1603-1608, Aug. 2010.
- [22] D. P. Borgers and W. P. M. H. Heemels, "Event-separation properties of event-triggered control systems," *IEEE Transactions on Automatic Control*, vol. 59, pp. 2644-2656, Oct. 2014.
- [23] Y. Batmani, M. Davoodi, and N. Meskin, "On design of nonlinear event-triggered suboptimal tracking controller," *Proc. of 4th International Conference on Control, Decision and Information Technologies (CoDIT)*, pp. 1048-1053, April 2017.
- [24] H. Khalil, *Nonlinear Systems*, Prentice Hall, 2002.
- [25] J. Kurzweil, "On the inversion of Lyapunov's second theorem on stability of motion," *Czechoslovak Mathematical Journal*, vol. 81, pp. 217-259, 1956.
- [26] A. Chaillet and A. Loria, "Necessary and sufficient conditions for uniform semiglobal practical asymptotic stability: Application to cascaded systems," *Automatica*, vol. 42, no. 11, pp. 1899-1906, 2006.
- [27] F. Espinosa, M. Salazar, D. Pizarro, and F. Valdes, "Electronics proposal for telerobotics operation of p3-dx units," *Remote and Telerobotics* (N. Mollet, ed.), ch. 1, InTech, Mar. 2010.

- [28] C. Santos, F. Espinosa, E. Santiso, and M. Mazo, "Aperiodic linear networked control considering variable channel delays: Application to robots coordination," *Sensors*, vol. 15, no. 6, p. 12454, 2015.
- [29] B. M. Kim and P. Tsiotras, "Controllers for unicycle-type wheeled robots: Theoretical results and experimental validation," *IEEE Transactions on Robotics and Automation*, vol. 18, pp. 294-307, Jun 2002.



Carlos Santos received his B.S. degree in Telecommunications Engineering in 2010 and an M.Sc. in Electrical Engineering in 2011, both from the University of Alcala, Spain, and a Ph.D. degree in Electronics in 2016. He is currently at the Department of Electronics of the University of Alcala with a Postdoctoral Research Contract. His research interest focuses on the field of fusion algorithms, trajectory generation for navigation in mobile robotics and varying-time sampling control techniques.

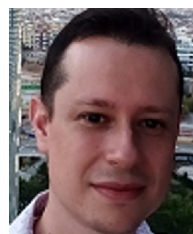


Felipe Espinosa received his M.S. degree (Polytechnics University of Madrid, Spain) and a Ph.D. degree (University of Alcala, Spain) in telecommunication, in 1991 and 1999 respectively. He became an Associate Professor in 2000 and a Full Professor in 2016 in the Electronics Department with the University of Alcala, regularly involved in electronic control

and automation subjects in the Post-Degree programme (Quality Awarded of the Education and Science Spanish Ministry). His current research interests include control, communication and sensorial systems applied to intelligent transportation systems, industrial automation and smart cities.



Enrique Santiso is an assistant professor at the Electronics Department, University of Alcala. He received his M.Sc. degree (Polytechnic University of Valencia, Spain) in 1996, and a Ph.D. (University of Alcala, Spain) in Telecommunications in 2003. His main research interest focuses on sensorial systems, control and electronics instrumentation.



David Gualda received his B.S. degree in Electronics Systems and an M.Sc. degree in Advanced Electronics System, from the University of Alcala (Spain), in 2009 and 2011, respectively; and a Ph.D. degree in Electronics in 2016. He is currently at the Department of Electronics of the University of Alcala with a Postdoctoral Research Contract. His main research interests are in

the areas of ultrasonic indoor location, signal processing and information fusion.

Publisher's Note Springer Nature remains neutral with regard to jurisdictional claims in published maps and institutional affiliations.